ANTIOXIDANTS & REDOX SIGNALING
Volume 14, Number 7, 2011

DOI: 10.1089/ars.2010.3163

ORIGINAL RESEARCH COMMUNICATION

Macrophage Migration Inhibitory Factor Provides Cardioprotection During Ischemia/Reperfusion by Reducing Oxidative Stress

Kiyokazu Koga,[1] Agnes Kenessey,[2] Saul R. Powell,[2] Cristina P. Sison,[3] Edmund J. Miller,[2] and Kaie Ojamaa[2]

Abstract

Macrophage migration inhibitory factor (MIF) is a multifunctional protein that exhibits an intrinsic thiol protein oxidoreductase activity and proinflammatory activities. In the present study to examine intracellular MIF redox function, exposure of MIF-deficient cardiac fibroblasts to oxidizing conditions resulted in a 2.3-fold increase ($p < 0.001$) in intracellular ROS that could be significantly reduced by adenoviral-mediated reexpression of recombinant MIF. In an animal model of myocardial injury by ischemia/reperfusion (I/R), MIF-deficient hearts exhibited higher levels of oxidative stress than did wild-type hearts, as measured by significantly higher oxidized glutathione levels (decreased GSH/GSSG ratio), increased protein oxidation, reduced aconitase activity, and increased mitochondrial injury (increased cytochrome *c* release). The increased myocardial oxidative stress after I/R was reflected by larger infarct size (INF) in MIF-deficient hearts versus wild-type (WT) hearts ($21 \pm 6\%$ vs. $8 \pm 3\%$ INF/LV; $p < 0.05$). *In vivo* hemodynamic measurements showed that left ventricular (LV) contractile function of MIF-deficient hearts subjected to 15-min ischemia failed to recover during reperfusion compared with WT hearts (LV developed pressure and $\pm$ dP/dt; $p = 0.02$). These data represent the first *in vivo* evidence in support of a cardioprotective role of MIF in the postischemic heart by reducing oxidative stress. *Antioxid. Redox Signal.* 14, 1191–1202.

Introduction

MACROPHAGE MIGRATION INHIBITORY FACTOR (MIF) is a pleiotropic cytokine that controls both innate and adaptive immune responses in both chronic and acute inflammatory diseases such as atherosclerosis, rheumatoid arthritis, and sepsis (3, 10, 34). In these pathologic conditions, inhibition of MIF proinflammatory activity by using small-molecule inhibitors or by immunodepletion has proven beneficial (9, 11, 38). In contrast, recent evidence suggests that secreted myocardial MIF acting in an autocrine/paracrine fashion can reduce ischemia/reperfusion injury by activating AMP kinase and suppressing JNK-mediated cell apoptosis (29, 35). These seemingly contradictory results suggest a complex role for this evolutionarily conserved molecule that can perhaps be partially reconciled by the recognition of distinct enzymatic activities of the MIF protein (4, 23, 43). Several studies suggest that the hydrophobic site of the MIF homotrimer is necessary for its proinflammatory function (2, 13), whereas its oxidoreductase activity may play a role in regulating cellular redox homeostasis (21, 22).

The redox function of MIF is mediated by a central CALC [Cys^{57}-Ala-Leu-Cys^{60}] motif that is similar to that found in other proteins with thiol-protein oxidoreductase (TPOR) activity, such as the thioredoxin protein superfamily (21, 27). *In vitro* analysis has shown that MIF acts as a disulfide reductase in its ability to reduce insulin disulfides by using either glutathione (GSH) or dihydrolipoamide as a co-substrate (22). Support for a role of MIF TPOR activity in cellular redox regulation has come from the use of mutants of MIF [in which the Cys^{60} has been mutated to serine (C60SMIF)] that lack oxidoreductase activity. Nguyen *et al.* (32) showed that overexpression of recombinant wild-type MIF (rMIF), but not the redox mutant C60SMIF, attenuated oxidative stress–induced apoptosis in cultured HeLa cells by maintaining cellular redox homeostasis. This effect was specific to intracellular overexpression of MIF and was not observed when cells were treated with exogenous rMIF. Their data also showed that when apoptosis was induced by mechanisms other than oxidative stress, intracellular overexpression of MIF was without effect. Furthermore, microinjection of rMIF into neurons prevented the increase in

[1]Elmezzi Graduate School of Molecular Medicine, [2]Center for Heart and Lung Research, and [3]Biostatistics Unit, The Feinstein Institute for Medical Research, North Shore-LIJ Health System, Manhasset, New York.

intracellular reactive oxygen species (ROS) after stimulation with angiotensin II, which did not occur with overexpression of the redox mutant C60SMIF (42).

The role of reactive oxygen and nitrogen species (ROS/RNS) in postischemic injury has been studied extensively, and the generation of these reactive molecules during ischemia and reperfusion has been well documented (1, 36, 49). Although the relative significance of reactive species in this process remains controversial, studies have consistently shown a causal relation between ROS/RNS generation during oxidative injury and myocardial stunning (5, 18, 30). Under normal conditions, the intracellular production and removal of reactive molecular species are tightly controlled by numerous redox-regulating systems, including Mn-superoxide dismutase, thioredoxin (Trx), thioredoxin reductase, glutaredoxin (Grx), peroxiredoxin (Prx), and glutathione peroxidase (1). However, during ischemia/reperfusion, excessive production of ROS and depletion or loss of intracellular antioxidant enzymes result in an oxidizing environment that can lead to lipid peroxidation, protein oxidation, and DNA damage, ultimately causing cell death (8, 47). The consequences of these effects on the myocardium are contractile dysfunction and arrhythmias (26). Whether MIF plays a meaningful role in reducing oxidative stress within the myocardium and in maintaining redox homeostasis in the setting of ischemic cardiac injury remains to be determined.

In light of the contradictory results of studies of MIF function as well as our own published studies showing a detrimental effect of MIF on cardiac function during sepsis (28, 38), we hypothesized that the oxidoreductase activity of intracellular MIF may play a protective role in the postischemic heart. In the current study using a model of ischemia and reperfusion (I/R) injury in wild-type and MIF-deficient animals, we provide evidence that MIF functions as an antioxidant to reduce postischemic myocardial tissue injury.

Materials and Methods

Animals

Animals used in these experiments were treated in accordance with National Institutes of Health *Guidelines for the Use and Care of Laboratory Animals* (DHHS Publication No. 85-23), and all study protocols were approved by the Animal Care and Use Committee of The Feinstein Institute. MIF-deficient (MIF KO) mice were developed on a mixed 129Sv×C57Bl/6 background (F1) and then backcrossed to C57Bl/6 (F7) at Charles River Laboratories, as described by Bozza *et al.* (6). No gross anatomic, histologic, or physiological abnormalities have been reported for these MIF-deficient mice when reared under standard laboratory conditions. Homozygous MIF KO mice used for this study were bred and maintained in the Center for Comparative Physiology at The Feinstein Institute. Male MIF KO mice were used at 10 to 12 weeks of age for *in vivo* studies, and similar aged wild-type C57Bl/6 male mice were purchased from Taconic Farms (Albany, NY).

Isolation and culture of cardiac fibroblasts

Cardiac fibroblasts were isolated from wild-type and MIF-deficient mice younger than 3 weeks by using published methods (12). In brief, the dissected hearts were treated 3 times with 0.025 to 0.05% collagenase (Worthington Biochemical Corp., Lakewood, NJ) for 30 min at 37°C with dispersion of the cells every 10 min. The cells were collected by centrifugation, suspended in DMEM containing 10% FBS, and seeded onto noncoated culture dishes. After overnight culture in an incubator containing 5% CO_2/room air at 37°C, nonadherent cells were removed by washing, and the adherent fibroblasts were cultured for two to three passages before experimentation. Microscopic examination of the cultures showed that >90% of cells were spindle-shaped, with few cobble-shaped endothelial cells and no cardiomyocytes after the first passage. Homogeneity of the cultures was further interrogated with Western blot analysis by using antibodies against prolyl-4-hydroxylase (P4HB; Abcam Inc., Cambridge, MA) and sarcomeric α-actinin (Sigma Aldrich, St. Louis, MO).

Recombinant adenovirus gene construction and transduction of cardiac fibroblasts

Replication-defective adenovirus containing the full-length coding sequence of mouse MIF was generated by first subcloning MIF cDNA into the pShuttle-CMV vector and then using homologous recombination in bacteria to generate recombinant adenovirus containing the MIF fragment by following the manufacturer's instructions (AdEasy Adenoviral Vector System; Stratagene, La Jolla, CA). The mouse MIF cDNA fragment was obtained with PCR amplification of full-length mMIF that had been initially cloned into pET11b plasmid (Novagen) (kindly provided by Dr. C.N. Metz) (4). Adenovirus expressing β-galactosidase (Ad-CMV-LacZ; Stratagene) was used for control cultures. All adenoviral constructs were verified with DNA sequencing. Recombinant adenoviruses were amplified by sequential infection of HEK-293 cells and purified by CsCl gradient ultracentrifugation, as previously described (19). The viral titer was determined by immunodetection of adenovirus hexon protein by using Adeno-X rapid titer kit (BD Biosciences, San Jose, CA).

Cardiac fibroblasts isolated from MIF KO hearts were seeded onto 96-well plates at $\sim 7\times10^3$ cells/well in 50 μl culture medium (DMEM, 10% FBS, 1% penicillin/streptomycin). After 48 h in culture, cells were washed and transduced with either Ad-MIF or Ad-LacZ in serum-free medium for 2 h, after which the medium was replaced with DMEM, 2% FBS. Adenovirus-mediated expression of MIF was measured after 48 h with Western blot analysis, and a multiplicity of infection (m.o.i.) of 200 was determined to produce intracellular MIF concentrations approximating that in wild-type fibroblasts. Oxidative-stress experiments were conducted 48 h after viral transduction.

Measurement of ROS generation by oxidative stress

Intracellular reactive species were quantified by using 2′,7′-dichlorodihydrofluorescein diacetate (DCF-DA) (20, 37). Cardiac fibroblasts isolated from wild-type or MIF KO mice were seeded onto 96-well plates (7×10^3 cells/well). In a subset of experiments, MIF KO cells were transduced with Ad-MIF or Ad-LacZ as described earlier. After 48 h in culture, the medium was changed to PBS containing 25 μ*M* DCF-DA. After 30-min incubation to allow cellular uptake of DCF-DA, the cells were washed extensively to remove extracellular DCF-DA and then treated with PBS or 1 m*M* hydrogen peroxide (H_2O_2 in PBS) for 30 min. at 37°C. Pilot studies showed

that treatment for 30 min at this dose was nontoxic and not saturating for ROS generation (data not shown). Oxidation of intracellular DCF was measured by excitation/emission maxima of 485 nm/530 nm by using a multiwell plate reader (CytoFluor II, Ramsey, MN). Data were normalized to the fluorescence measured in control PBS-treated cells. Cellular morphology and fluorescence produced in response to H_2O_2 treatment were visualized microscopically (Zeiss Axiovert 200M; Carl Zeiss, Thornwood, NY). Measurement of cell viability in response to 30-min H_2O_2 treatment was determined by using the trypan blue dye (0.7%) exclusion method. Cells were counted by using a hemocytometer, and the number of viable cells was expressed as a percentage of total cell number.

Myocardial ischemia/reperfusion protocol

The ischemia/reperfusion (I/R) protocol was performed essentially as described by Jones *et al.* (17). In brief, mice were anesthetized by intraperitoneal administration of ketamine (50 mg/kg) and sodium pentobarbital (50 mg/kg). Mice were orally intubated with polyethylene-60 tubing and mechanically ventilated with 100% oxygen by using a rodent ventilator (Minivent model 845; Harvard Apparatus, Holliston, MA) with a respiratory rate of 170 breaths/min and a tidal volume of 170 μl. Sodium heparin (200 unit/kg) was delivered by intraperitoneal injection 10 min before coronary artery ligation. A left paramedian thoracotomy was performed, and the left coronary artery (LCA) was visualized and ligated with 7-0 silk suture around 2-mm polyethylene-10 (PE-10) tubing to prevent crush injury to the vessel. The LCA was occluded for either 15 or 30 min, followed by removal of the suture and reperfusion for the periods indicated in the analysis section. Mice were ventilated with 100% O_2 until fully recovered from anesthesia. Assessments of infarct size were performed in a blinded fashion.

Myocardial infarct–size determination

Determination of infarct size was performed as previously published (17). At the end of the reperfusion period, mice were anesthetized and mechanically ventilated as described earlier. The right carotid artery was exposed, and a catheter (PE-10 tubing) was inserted into the artery for injection of Evans blue dye (Sigma Aldrich). A left thoracotomy was performed, and the LCA was ligated in the same location as previously, and a bolus of 0.7 ml of 7% Evans blue dye solution was injected into the circulation via the carotid-artery catheter to delineate the nonischemic heart tissue from the area at risk (AAR) . Within 2 min, the heart was excised and sectioned along the short axis into five or six 1-mm slices that were subsequently incubated in 2,3,5-triphenyl-tetrazolium chloride solution (TTC, 1% in PBS; Sigma Aldrich), for 10 min at 37°C to delineate the viable and nonviable myocardium within the AAR. Each slice was weighed and then scanned for measurement of the area of infarction (TTC negative), AAR (Evans blue negative), and total left ventricular (LV) area by using computer-assisted planimetry (NIH ImageJ, Bethesda, MD). These distinct areas were multiplied by the weight of each section, and the summation from the sections equaled the total infarct area or the total AAR, as described by Jones *et al*. (17). Infarct size was expressed as a percentage of the AAR or the total LV.

In vivo *hemodynamic analysis*

Left-ventricle function during ischemia and reperfusion was measured *in vivo*. Wild-type or MIF KO mice were anesthetized and mechanically ventilated as described earlier. After exposing the heart by thoracotomy, a 1.4-Fr Millar catheter (SPR-671; Millar Instruments, Houston, TX) was inserted into left ventricle through the apex. Left ventricle pressure was continuously recorded during a 5-min preischemic period, followed by 15-min LCA occlusion and 20 min of reperfusion by using surgical procedures described earlier. Data were collected by using PowerLab 8/30 acquisition system (AD Instruments; Colorado Springs, CO), and data from 200 or more cardiac cycles for each time point were analyzed with LabChart Pro software.

Preparation of LV tissue homogenate, cytosolic and mitochondrial fractions

Hearts were excised after 15-min ischemia followed by 5-min reperfusion, and the LV free wall was isolated and immediately frozen in liquid nitrogen and stored at −80°C. For analysis, frozen tissue was homogenized in 15 volumes of ice-cold homogenization buffer (10 m*M* Tris HCl, pH 7.4, 0.25 *M* sucrose, and 30 m*M* sodium citrate) by using a motor-driven mortar and Teflon pestle. The LV tissue homogenate was then centrifuged at 1,000 *g* for 10 min at 4°C, and the resulting supernatant collected and centrifuged at 10,000 *g* for 30 min at 4°C to obtain the cytosolic fraction. The mitochondrial fraction was prepared by resuspending the 10,000 *g* pellet in homogenization buffer without sucrose. Protein concentrations were determined with the Micro BCA assay (Pierce, Rockford, IL). These mitochondrial and cytosolic fractions were used for aconitase activity and protein carbonyl measurements.

Mitochondrial injury measured with cytochrome c *release*

Mitochondrial release of cytochrome *c* into the cytosol was measured in the postmitochondrial fraction obtained by centrifugation of the 10,000 *g* supernatant fraction at 100,000 *g* for 1 h at 4°C and recovering the supernatant. Absence of mitochondrial contaminants in this fraction was confirmed by immunoblotting with anti-cytochrome *c* oxidase (COX IV) antibody (Cell Signaling, Danvers, MA), an inner mitochondrial membrane protein (Fig. 5A). To ascertain that tissue freezing did not cause excessive mitochondrial damage, cytochrome *c* release was measured in postmitochondrial fractions prepared from both fresh and frozen tissue and found not to be different. Our preliminary experiments showed that significant cytochrome *c* was released after 15-min ischemia, and that the amount released after 5-min reperfusion was equivalent to that released at 30- and 60-min reperfusion. Therefore, to minimize animal use, we used the same hearts subjected to 15-min ischemia followed by 5-min reperfusion that were processed for aconitase and protein carbonyl analyses. Protein concentration of the postmitochondrial fraction was determined with the Micro BCA assay, and 2 μg protein was used to detect cytochrome *c* with Western blotting methods (anti-cytochrome *c* antibody; BD Pharmingen, San Jose, CA).

Immunoquantitation of GAPDH was used for normalization (anti-GAPDH antibody; Cell Signaling). HRP-conjugated

secondary antibody signal was developed by using chemiluminescence reagent (Perkin Elmer) and detected by exposure to x-ray film. Protein band intensity was quantified with laser-scanning densitometry by using Quantity One 4.2.2. software (GS-800 Densitometer; BioRad, Hercules, CA). Data are expressed as arbitrary densitometric units.

Indicators of oxidative stress

Protein carbonyl content in cytosolic and mitochondrial compartments. Dithiothreitol (DTT; 25 m*M* final) was added immediately to an aliquot of the LV homogenate to prevent oxidation. The homogenate was then fractionated to obtain mitochondrial and cytosolic fractions, as described earlier, and protein concentrations were measured by using the Bradford assay (Pierce). The extent of protein oxidation was determined by reaction with 2,4-dinitrophenylhydrazone (DNPH) according to a commercially available kit (OxyBlot; Millipore, Bedford, MA). Oxidized proteins were identified by immunodetection of the DNPH-derivatized carbonyl groups in proteins (2.5 μg) that had been separated with 10% SDS-PAGE and transferred to nitrocellulose membrane. Immunoreactive protein bands were detected with chemiluminescence exposure of x-ray film, and proteins were quantified with laser-scanning densitometry, as described earlier. Quantitation of protein carbonyls in the mitochondrial fraction included those from 40 to 80 kDa, whereas protein carbonyls from 50 to 80 kDa were quantified in the cytosolic fraction to exclude the prominent sarcomeric-actin band at 43 kDa.

Tissue aconitase activity. Aconitase activity was measured in 7 μg and 10 μg protein of mitochondrial and cytosolic fractions, respectively, by using a commercially available kit essentially as recommended by the manufacturer (Cayman Chemical, Ann Arbor, MI).

Tissue GSH/GSSG ratio. Left ventricular concentrations of GSH and GSSG were determined with the established glutathione reductase/DTNB recycling procedure by using a commercially available kit (Calbiochem, San Diego, CA). Hearts were excised either before ischemia, immediately after 15 min of ischemia, or after 60 min of reperfusion. Hearts were washed by retrograde perfusion of cold PBS, and the LV free wall was isolated, rapidly frozen in liquid nitrogen, and stored at -80°C. The frozen tissue was homogenized in ice-cold MES buffer [0.2 *M* 2-(*N*-morpholino)ethanesulfonic acid, 0.05 *M* phosphate, and 1 m*M* EDTA, pH 6.0] followed by deproteination in metaphosphoric acid (Sigma Aldrich). Processed samples were stored at -80°C until assayed. Before analysis, samples were neutralized, and total GSH was determined. GSSG content was measured by first derivatizing GSH in the samples with 2-vinylpyridine.

Baseline redox activities in MIF KO hearts

Immunoblot analysis. LV tissue from 10- to 11-week-old wild-type and MIF KO mice was prepared as described earlier, and immunoblot analysis was used to determine basal levels of expression of key redox-regulatory proteins including thioredoxin I (Abcam Inc., Cambridge, MA), peroxiredoxin I and II (Santa Cruz Biotechnology, Inc., Santa Cruz, CA). Anti-MIF antibodies (Abcam) were used to ascertain MIF gene deletion in MIF KO mice, and anti-GAPDH antibodies (Sigma Aldrich) were used for immunoblot normalization.

Enzymatic activities. Activities of cytosolic SOD, catalase, glutathione peroxidase, and glutathione reductase were measured in LV tissue by using commercially available assay kits and following the manufacturer's recommendations for tissue preparation and analysis (Cayman Chemical Co., Ann Arbor, MI).

Statistical analysis

All data are expressed as mean $\pm$ standard error of the mean (SEM). Sigma Stat software (Systat Software, Chicago, IL) and SAS 9.1 (Cary, NC) were used for data analyses. Comparisons between groups were carried out by using Student's *t* test or the Mann–Whitney test, as appropriate. ANOVA was used to compare multiple groups, and adjusted pairwise comparisons were carried out to determine which groups differed from one another. Within-group differences were compared by using the paired *t* test or the Wilcoxon Signed Rank test, as appropriate. A value of $p < 0.05$ was considered statistically significant.

Results

Increased ROS in MIF-deficient cardiac fibroblasts exposed to oxidative stress

Initial experiments were designed to determine whether intracellular MIF played a role in maintaining redox homeostasis during oxidative stress in cardiac cells based on the intrinsic oxidoreductase activity of MIF (21, 22). Cardiac fibroblasts isolated from WT and MIF KO hearts were expanded in culture to obtain sufficient numbers of cells for experimentation. As shown in Fig.1A and C, cardiac fibroblasts at the third passage in culture were a relatively homogeneous population of spindle-shaped cells that expressed prolyl-4-hydroxylase (P4HB), a fibroblast protein marker (46), and did not express myocyte-specific α-actinin, as shown for mouse whole-heart homogenate. Furthermore, immunoblot analysis verified that cultured fibroblasts isolated from MIF KO hearts did not express MIF protein (Fig. 1E). To measure reactive species generation in response to oxidative-stress conditions, fibroblasts were preloaded with the ROS-sensitive fluorescence indicator, DCF-DA, and then treated with H_2O_2 for 30 min. Preliminary dose–response experiments with concentrations of H_2O_2 between 0.025 m*M* and 1 m*M* showed that the cellular response to 1 m*M* H_2O_2 was not saturating at 30 min, fell within the linear part of the response curve, and did not affect cell viability of either WT or MIF KO cells (Fig. 1B). Microscopic imaging showed that the DCF-loaded cultured fibroblasts treated with 1 m*M* H_2O_2 generated green fluorescence (Fig. 1C), and quantitation of the fluorescence (Fig. 1D) showed that the amount of DCF-sensitive oxidative species generated in response to H_2O_2 was significantly greater in MIF-deficient cells than in WT fibroblasts (2.71 ± 0.18 vs. 1.66 ± 0.13-fold increase of PBS control, respectively).

Reexpression of MIF protein in MIF-deficient fibroblasts with an adenoviral delivery approach was used to determine whether MIF alone was sufficient to reduce oxidative stress in response to H_2O_2 treatment. The immunoblot in Fig. 1E shows

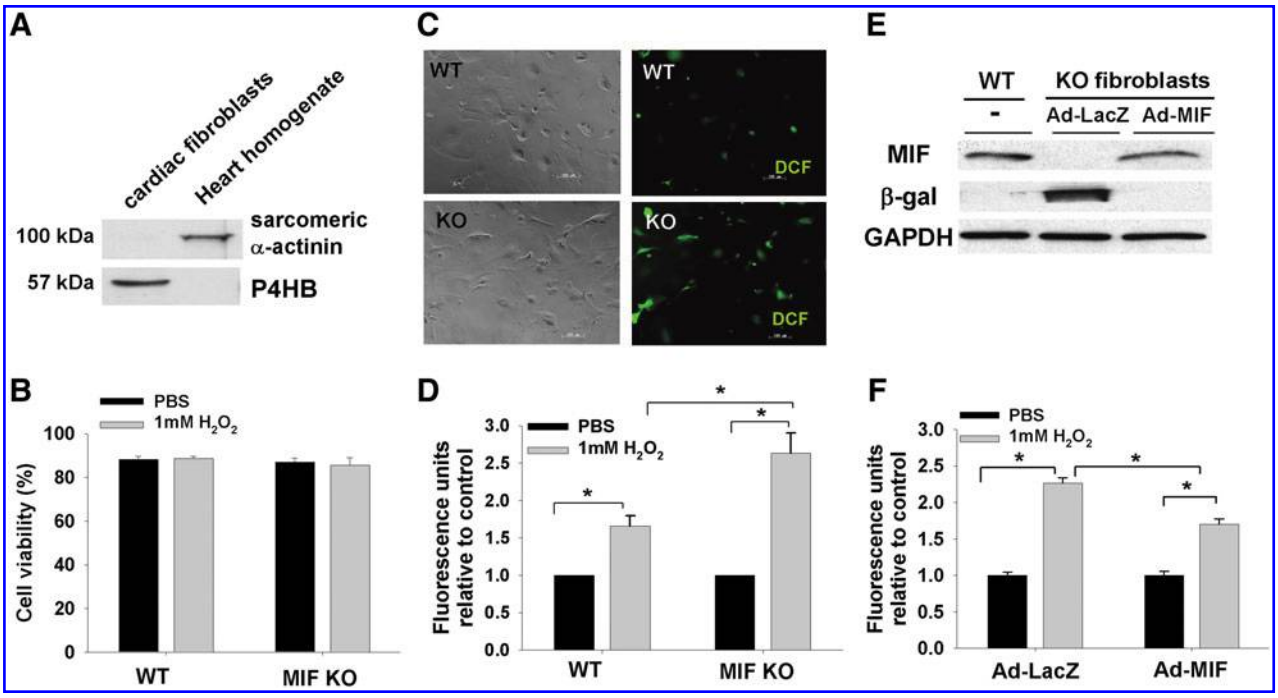

FIG. 1. Increased oxidative stress response in MIF-deficient cardiac fibroblasts. (A) Immunoblot of cardiac fibroblast lysate showing presence of fibroblast marker, P4HB, and absence of myocyte marker, sarcomeric α-actinin. Mouse-heart homogenate is shown for comparison. **(B)** Viability of cultured cardiac fibroblasts isolated from WT or MIF KO hearts after exposure to 1 m*M* H_2O_2 for 30 min, measured with trypan blue exclusion. **(C)** Microscopic images of WT and KO cultured cardiac fibroblasts preloaded with DCF-DA and then treated with H_2O_2, as described in Materials and Methods. *Left panels*, Phase-contrast images; *right panels*, green fluorescence detected at excitation/emission of 485 nm/530 nm, which indicates oxidation of DCF in response to H_2O_2 treatment. **(D)** Bar graph shows quantitation of DCF oxidation in cardiac fibroblasts treated with PBS or 1 m*M* H_2O_2. Results are expressed relative to control PBS-treated cells. Results are expressed as mean ± SEM; $n = 5$ per condition. *$p < 0.001$ between groups is indicated by the line. Data are representative of three separate cell isolations. **(E)** Immunoblot of MIF KO cardiac fibroblast lysates showing MIF or β-galactosidase expression, 48 h after transduction with Ad-MIF or Ad-LacZ. MIF expression in WT fibroblasts is shown for comparison. GAPDH was used for normalization. **(F)** Intracellular ROS generation in response to H_2O_2 treatment in MIF-deficient cardiac fibroblasts 48 h after Ad-LacZ or Ad-MIF transduction. Results are expressed as mean ± SEM; $n = 4$ to 5 per condition. *$p < 0.001$ between groups indicated. Data are representative of similar experiments from two separate cell isolations. (For interpretation of the references to color in this figure legend, the reader is referred to the web version of this article at www.liebertonline.com/ars).

that adenoviral-mediated delivery of recombinant MIF into MIF KO fibroblasts produced similar levels of MIF protein expression to those of wild-type cells. Also shown are MIF KO fibroblasts transduced with the control adenoviral vector expressing β-galactosidase (Ad-LacZ). As described earlier, these fibroblasts were preloaded with DCF-DA and then treated with H_2O_2 for 30 min. The oxidative-stress response as measured by ROS-activated DCF fluorescence was significantly lower in fibroblasts in which MIF had been reexpressed (Ad-MIF) compared with MIF-deficient cells (Ad-LacZ) (1.70 ± 0.07 vs. 2.26 ± 0.07-fold increase of PBS controls) (Fig. 1F). The observation that reexpression of MIF in KO cells reduced the oxidative response to that observed in WT cells (Fig. 1D) supports the hypothesis that MIF alone is sufficient to diminish intracellular ROS content and supports its role in regulating redox homeostasis in response to oxidative stress.

Baseline level of expression and activity of redox proteins in WT and MIF KO hearts

To determine whether the observed oxidative-stress response in cultured MIF-deficient cardiac cells extended to is-

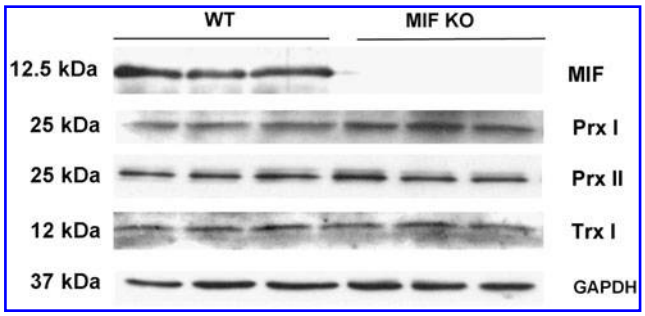

FIG. 2. Baseline expression of redox-regulatory proteins in MIF-deficient and WT hearts. Immunoblot analysis of heart lysates shows similar levels of expression of redox proteins, peroxiredoxin I and II (Prx I, II), and thioredoxin I (Trx I) in MIF KO and WT mice. GAPDH was used for normalization. MIF KO hearts show complete absence of immunoreactivity with anti-MIF antibody.

Table 1. Baseline Activity of Redox Regulatory Enzymes in WT and MIF KO Hearts

	WT	*MIF KO*
Cytosolic SOD (U/mg protein)	35.31 ± 2.70	39.02 ± 0.66
Catalase (nmol/min/mg protein)	59.60 ± 1.88	53.22 ± 2.49
Glutathione peroxidase (nmol/min/mg protein)	19.29 ± 1.13	22.43 ± 1.34
Glutathione reductase (nmol/min/mg protein)	300.7 ± 11.3	288.5 ± 5.87

Data are expressed as mean ± SEM; $n = 4$–5 per group; no statistical differences were found between groups.

chemic injury *in vivo*, we first assessed the effects of genetic MIF deficiency on expression and activity of other key redox-regulatory proteins in myocardial tissue under normal physiologic conditions. The representative immunoblot in Fig. 2 illustrates that expression levels of peroxiredoxin I and II (Prx I, II), and thioredoxin I (Trx I) were not different between MIF KO and WT hearts. We also showed that the myocardial enzymatic activities of catalase, cytosolic superoxide dismutase (SOD), and glutathione peroxidase and reductase were not significantly different between the two groups of animals (Table 1). These data lend support to a unique role of MIF in cellular redox homeostasis, although it cannot be completely ruled out that other unexamined redox homeostatic mechanisms may be altered to compensate for the genetic loss of MIF in the heart.

MIF deficiency leads to increased LV infarct size after ischemia/reperfusion

To study the role of intracellular MIF on the oxidative-stress response in the myocardium *in vivo*, we subjected hearts from MIF-deficient and wild-type mice to ischemia/reperfusion injury. In all experiments, the area at risk (AAR) expressed as a percentage of the LV was similar for MIF-deficient and wild-type mice, indicating that the experimentally induced ischemic injury was comparable (AAR/LV in Fig. 3B–D). Notably, the infarct size (INF) was significantly greater in the MIF-deficient hearts when subjected to 15-min ischemia followed by 24-h reperfusion ($21.1 \pm 6.0\%$ vs. $8.4 \pm 2.6\%$, INF/AAR; $p < 0.05$; $10.9 \pm 3.2\%$ vs. $4.5 \pm 1.4\%$, INF/LV; $p < 0.05$) (Fig. 3B.). This effect of MIF-deficiency was observed as early as 4 h of reperfusion ($31.3 \pm 4.6\%$ vs. $15.5 \pm 4.9\%$, INF/AAR; $p < 0.05$; $17.6 \pm 3.2\%$ vs. $9.4 \pm 3.0\%$,

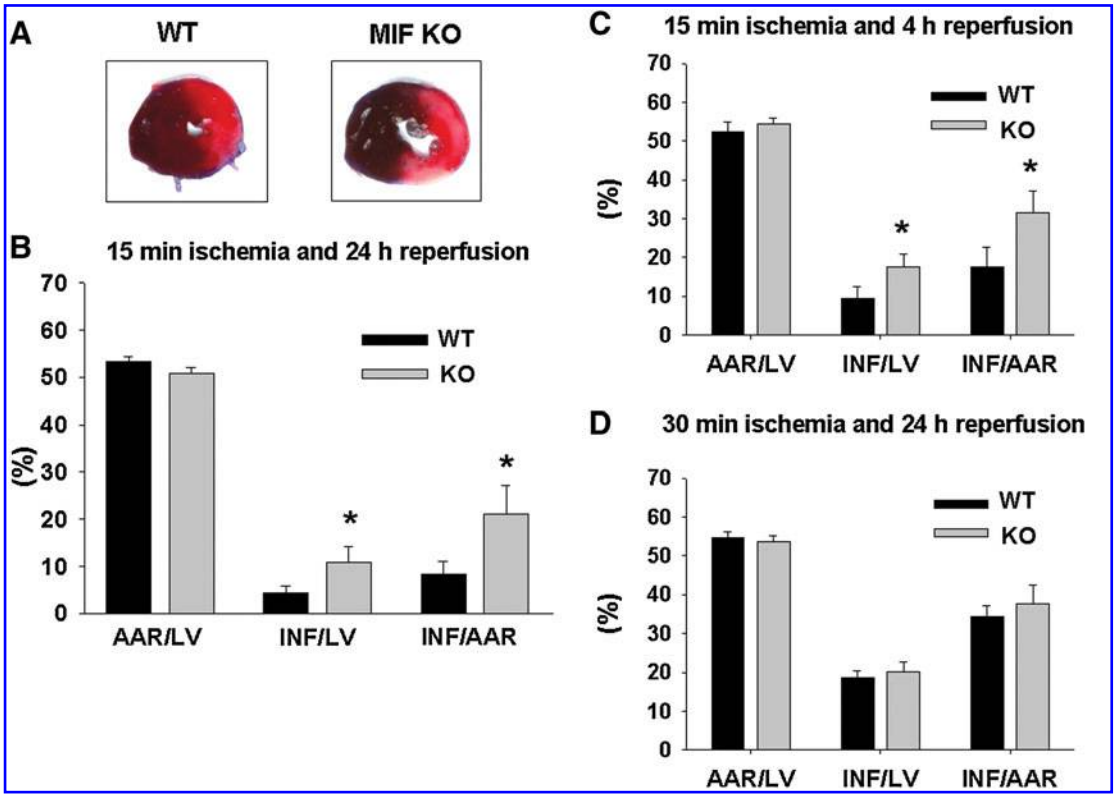

FIG. 3. Increased myocardial infarct size in MIF KO versus WT mice after I/R. (A) Representative heart slices from WT and MIF KO mice after 15-min left coronary artery occlusion followed by 24 h of reperfusion. Tissue area not stained by Evans blue dye indicates ischemic area at risk (AAR), whereas viable tissue is stained red with TTC. The white or non–TTC-stained area indicates infarcted tissue (INF). Bar graphs represent quantitation of the infarct area (INF) expressed as a percentage of the AAR (INF/AAR) or total left ventricular area (INF/LV), as described in Materials and Methods. Data are expressed as mean ± SEM. **(B)** Results are from hearts subjected to 15-min ischemia/24 h reperfusion. *$p < 0.05$ vs. WT; $n = 8$ WT, 10 MIF KO. **(C)** Hearts subjected to 15-min ischemia/4-h reperfusion. *$p < 0.05$ vs. WT; $n = 8$ WT, 9 MIF KO; and **(D)** 30-min ischemia/24-h reperfusion; $n = 11$ WT, 10 MIF KO. (For interpretation of the references to color in this figure legend, the reader is referred to the web version of this article at www.liebertonline.com/ars).

Table 2. *In vivo* Hemodynamic Measurements Recorded in Wild-type and MIF KO Mice

	WT	*MIF KO*
HR (beats/min)	527 ± 21	518 ± 36
Max-Min pressure (mm Hg)	66 ± 2	62 ± 4
LVEDP (mm Hg)	1.3 ± 0.4	1.2 ± 0.4
Max dP/dt (mm Hg/s)	5,230 ± 454	4,610 ± 496
Min dP/dt (mm Hg/s)	−5,460 ± 535	−5,340 ± 953

Data are expressed as mean ± SEM; $n = 5$–7 mice/group. No statistical differences were found between groups.

INF/LV; $p < 0.05$). In contrast, when the period of ischemia was extended to 30 min followed by 24-h reperfusion, the infarct size of the WT hearts was increased to that observed in MIF-deficient hearts (34.3 ± 2.8% vs. 37.6 ± 4.8%, INF/AAR), suggesting that the protection afforded by MIF was dependent on the extent of ischemia.

MIF deficiency impairs postischemic recovery of cardiac function

In vivo measures of cardiac function in MIF-deficient mice were similar to those in wild-type animals at baseline (Table 2). Fig. 4 shows hemodynamic measurements recorded continuously in anesthetized mice 5 min before ischemia, and during 15 min of ischemia followed by 20 min of reperfusion. Within the first minute of ischemia, LV developed pressure (max-min pressure) was significantly reduced from the preischemic value in both WT and MIF KO mice ($p = 0.03$), and significant impairments in the rates of LV pressure development (min dP/dt, max dP/dt) were recorded. During the 20-min period of reperfusion, only the WT mice exhibited significant ($p = 0.02$) recovery of cardiac function, whereas all measures of contractile function in the MIF-deficient mice remained unchanged from that recorded during the ischemic period (Fig. 4).

Increased mitochondrial cytochrome c release in MIF-deficient hearts

Release of cytochrome *c* from the mitochondria is an indicator of the severity of myocardial ischemic injury and a marker of apoptosis. As shown by the immunoblot in Fig. 5A, the absence of the mitochondrial inner membrane protein, cytochrome oxidase (COX IV) in the cytosolic fraction verified that any cytochrome *c* detected in this fraction represented specific mitochondrial cytochrome *c* release. The representative immunoblot in Fig. 5B shows that myocardial injury as

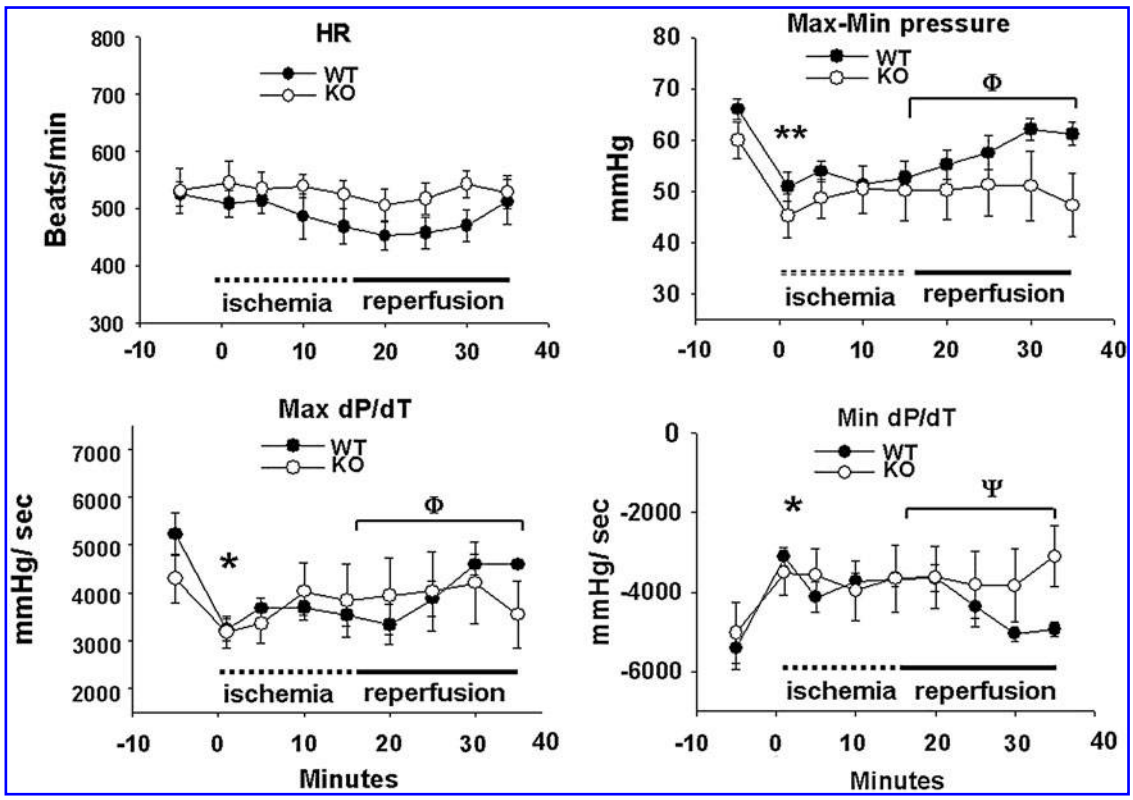

FIG. 4. LV contractile function of MIF-deficient hearts fails to recover after ischemia. *In vivo* hemodynamic measurements recorded continuously and calculated every 5 min starting 5 min before LCA occlusion for 15 min of ischemia followed by 20 min of reperfusion. Measurements at each time point represent the mean ± SEM of six WT and seven MIF KO mice. Heart rates (HRs) from WT and MIF KO mice showed no significant changes. LV developed pressure (Max-Min pressure) decreased significantly within 1 min of ischemia (**$p = 0.03$ vs. preischemia for WT and KO); Φ$p = 0.02$, WT vs. KO during reperfusion. Max and Min dP/dt were significantly reduced during ischemia (*$p = 0.03$ vs. preischemia, WT only). During reperfusion, Max dP/dt differed between WT and KO at Φ$p = 0.02$; and Min dP/dt at $^{\Psi}p = 0.055$, WT versus KO (Mann–Whitney test).

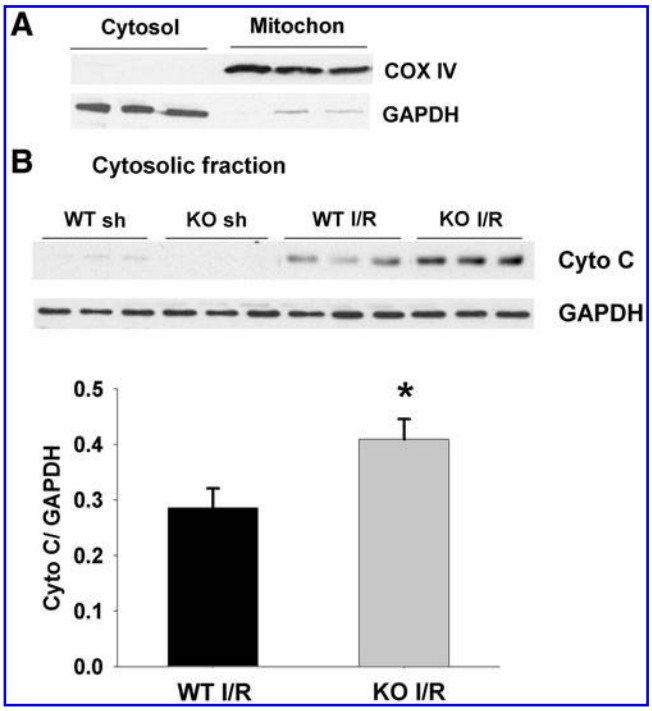

FIG. 5. Increased mitochondrial release of cytochrome *c* in MIF KO hearts after I/R. (A) Immunoblot analysis showing that expression of the mitochondrial inner membrane protein, cytochrome *c* oxidase IV (COX IV), is limited to the mitochondrial fraction, whereas GAPDH is specific to the cytosolic fraction. **(B)** Release of cytochrome *c* (Cyto C) from the mitochondria after I/R (15-min ischemia/5-min reperfusion) or sham (sh) operation was determined by immunoblot analysis of the cytosolic fraction prepared from the AAR, as described in Materials and Methods. Quantitation of Cyto C normalized to GAPDH in the Western blot is depicted in the bar graph. $*p < 0.05$ vs. WT. Data are expressed as mean ± SEM; $n = 4$ mice per group. Data are representative of two separate experiments.

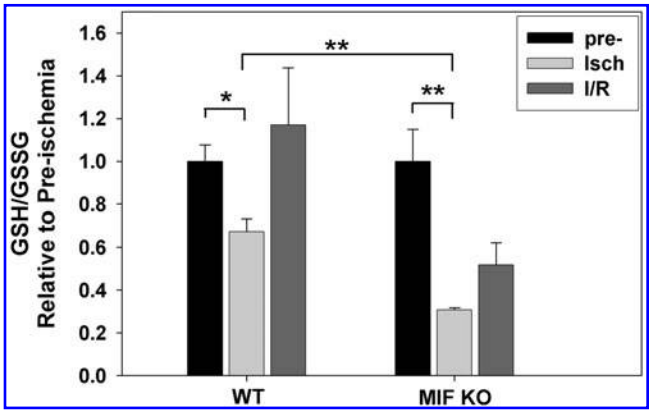

FIG. 6. Increased oxidized glutathione in hearts of MIF KO mice after ischemic injury. Glutathione (GSH) and glutathione disulfide (GSSG) were measured in the ischemic myocardium of WT and MIF KO mice subjected to 15-min ischemia alone (Isch) or followed by 60 min of reperfusion (I/R). Bar graph shows the data expressed as the GSH-to-GSSG ratio compared with values obtained from preischemic LV tissue (pre-). $*p < 0.01$; $**p < 0.001$. Results are expressed as mean ± SEM of three to five mice per condition.

indicated by the presence of cytochrome *c* in the cytosolic fraction was negligible in sham-operated WT and MIF KO mice, whereas cytochrome *c* released from mitochondria in MIF KO hearts was significantly greater ($p < 0.05$) than that in WT hearts after I/R, suggesting greater mitochondrial damage. Densitometric quantitation of the immunoblots is indicated in the bar graph.

MIF deficiency increases myocardial oxidative stress in vivo

To test further the hypothesis that MIF functions to regulate redox homeostasis, we measured several indicators of oxidative stress in WT and MIF KO hearts after ischemia/reperfusion. In the first series of experiments, the myocardial concentrations of reduced glutathione (GSH) and oxidized glutathione disulfide (GSSG) measured after 15 min of ischemia and after 60 min of reperfusion were compared with the preischemic values. Total glutathione (reduced and oxidized) content in the preischemic hearts was similar in WT and MIF KO mice (18.4 ± 0.3 ng/mg vs. 18.1 ± 0.7 ng/mg protein, respectively). As shown in Fig. 6, oxidation of GSH to GSSG was increased significantly in both groups of mice after 15 min of ischemia, although the decrease in the GSH/GSSG ratio was significantly ($p < 0.001$) greater in the MIF KO than in the WT hearts. Furthermore, after 60 min of reperfusion, the GSH/GSSG ratio in the WT hearts returned to preischemic levels, whereas the GSH/GSSG ratio in MIF KO hearts remained low, suggesting that the redox-regulatory activity of MIF was important in maintaining normal myocardial redox potential during ischemia and reperfusion.

A downstream consequence of increased intracellular reactive molecular species is protein oxidation. Therefore, the presence of carbonyl groups on proteins isolated from both mitochondrial and cytosolic fractions was used to estimate the extent of protein oxidation in response to ischemia/reperfusion. Based on published data (7) and our preliminary experiments, protein carbonylation peaked within 5 min of reperfusion. As illustrated by the immunoblots in Fig. 7A and B and quantified with densitometry (bar graphs), the presence of protein carbonyls in both mitochondrial and cytosolic fractions after 15 min of ischemia followed by 5 min of reperfusion was significantly higher ($p < 0.05$) in the MIF KO hearts than in the WT hearts (13.4 ± 1.6 vs. 7.1 ± 1.7; 40 kDa to 80-kDa mitochondrial proteins; 13.6 ± 0.8 vs. 10.4 ± 0.9; 50 kDa to 80-kDa cytosolic proteins). The abundant cytosolic DNPH-derivatized protein at 43 kDa includes myofibrillar actin that we have previously shown to be susceptible to oxidation (39). We have excluded this protein band to measure more accurately the differences in oxidation of other higher-molecular-weight cytosolic proteins in Fig. 7B. These data support a role of MIF in reducing overall protein oxidation in response to ischemia/reperfusion.

As a further indicator of oxidative stress in the heart, the enzymatic activity of aconitase was measured because its activity is dependent on its iron–sulfur cluster $[4Fe\text{-}4S]^{2+}$ that can be inactivated by superoxide. Based on published data showing the time course of maximal inhibition of aconitase activity (7), we measured cytosolic and mitochondrial aconitase activity after 15-min ischemia followed by 5-min

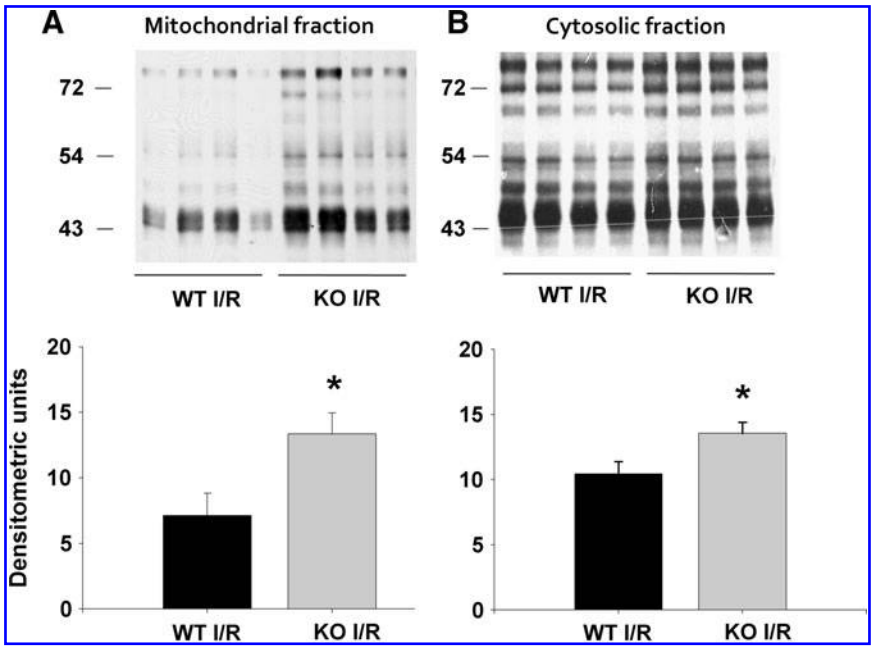

FIG. 7. Increased protein oxidation in hearts of MIF KO mice after I/R. After exposure to coronary artery occlusion for 15 min followed by 5-min reperfusion (I/R), the LV free wall (area at risk) was processed for immunoblot determination of protein carbonylation in both mitochondrial **(A)** and cytosolic **(B)** fractions, as described in Materials and Methods. Bar graphs show quantitation of the immunoblot DNPH-conjugated proteins between 40 and 80 kDa in the mitochondrial fraction, and between 50 and 80 kDa in the cytosolic fraction, as depicted in the immunoblots. Data are expressed as mean ± SEM. $*p < 0.05$ vs. WT; $n = 4$ per group.

reperfusion. As shown in Fig. 8, cytosolic aconitase activity was significantly inhibited in the hearts of MIF KO mice after I/R compared with sham-operated animals, whereas no inhibition of enzymatic activity was observed in the WT hearts. Aconitase activity in the mitochondrial fraction was not altered after ischemia/reperfusion in either WT or MIF KO hearts (data not shown).

Discussion

Although MIF has been described primarily as a pleiotropic cytokine that controls both innate and adaptive immune responses, this versatile protein may also play a role in maintaining cellular redox homeostasis (21, 22, 32, 33). In support of this latter function, the results of the present study show that MIF redox activity can reduce cellular oxidative stress and thus minimize injury in the postischemic heart. To demonstrate that MIF has intracellular redox potential, exposure of MIF-deficient cardiac fibroblasts to oxidizing conditions resulted in an increase in intracellular ROS that was significantly reduced by reexpression of recombinant MIF. The *in vivo* series of experiments were designed to show that this antioxidant property of MIF mitigated postischemic injury by reducing oxidative stress in the myocardium. This conclusion was supported by the recovery of the GSH/GSSG ratio to preischemic values in WT but not in MIF-deficient hearts during reperfusion.

Second, we showed that the increased oxidative environment in the MIF-deficient myocardium resulted in significantly greater oxidation of both mitochondrial and cytosolic proteins, as measured by formation of protein carbonyls, inhibition of aconitase enzymatic activity, and mitochondrial injury.

Third, continuous *in vivo* hemodynamic recording of LV pressure showed significant recovery of function during the reperfusion period in WT but not in MIF KO mice. Taken together, these data support an integral role for MIF in protecting the cellular milieu from excessive oxidative conditions.

The recognition that MIF exhibits oxidoreductase activity by a cysteine thiol–mediated mechanism has been reported by several investigators (21, 22, 24). Interestingly, this combined function of cytokine-like activity and enzymatic redox activity had already been reported for thioredoxin and cyclophilin (24, 40, 44). The reducing potential of a 16-amino-acid peptide sequence within MIF containing the CXXC thiol protein oxidoreductase motif was determined to be −258 mV (32), which is similar to the reducing potential of the oxidized form of thioredoxin of −270 mV (25). The importance of the MIF redox function in relation to other members of the thioredoxin superfamily is presently unclear. Thioredoxins (Trxs) and glutaredoxins are principal antioxidant systems within the cardiomyocyte that protect the myocytes from oxidative stress (1, 31). Although we did not observe significant changes

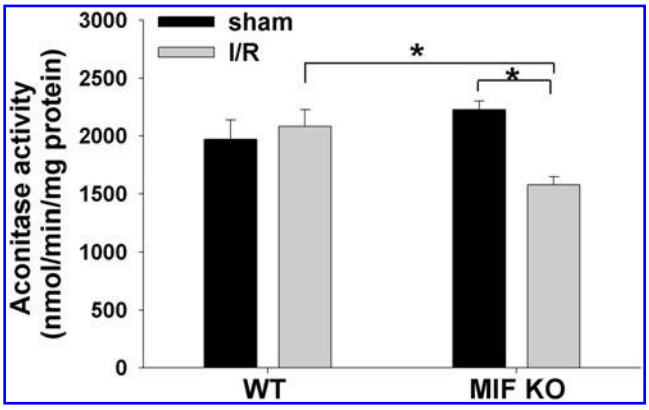

FIG. 8. Reduced aconitase activity in MIF KO hearts after I/R. Bar graph shows cytosolic aconitase activity in the LV free wall after 15-min left coronary artery occlusion followed by 5-min reperfusion (I/R) or sham operation in WT and MIF KO mice. $*p < 0.05$. Data are expressed as mean ± SEM of four mice per condition.

in expression or enzymatic activity of key redox proteins in the MIF-deficient hearts under normal conditions, we cannot completely rule out the possibility that other intracellular redox pathways compensate for the loss of MIF in these mice. For example, Kondo *et al.* (24) reported significantly higher intracellular Trx protein in $CD4^+$ T cells derived from MIF-deficient mice than from wild-type mice.

In the present study, the significance of MIF redox function could be seen by its cardioprotective effect during relatively short periods of ischemia (15 min), whereas longer ischemic times (30 min) provided little or no protection. Studies have shown that mitochondrial oxidant generation increases during cellular hypoxia, and that the magnitude of the oxidant stress contributes to the extent of cell death during reperfusion (36, 49). Furthermore, other injurious mechanisms contribute to tissue injury during ischemia, including reduced ATP, $NADH/NAD^+$, acidosis, and calcium overload (16). Therefore, the effectiveness of MIF oxidoreductase activity in our studies likely illustrates its role as only one component in an elaborate molecular network that functions to maintain intracellular redox homeostasis in the myocardium (27).

The intracellular redox function of MIF may play a complementary role to its reported extracellular activity as an autocrine/paracrine factor. Miller *et al.* (29) showed that MIF treatment of isolated papillary muscles increased phosphorylation of AMP-activated protein kinase (AMPK), and stimulated GLUT-4 translocation to the membrane, leading to increased glucose uptake and metabolism, thus potentially preventing cardiac dysfunction and reducing myocardial infarct size. The role of extracellular MIF has been further defined by these authors in recent studies showing that treatment of the isolated perfused MIF-deficient heart with recombinant MIF (rMIF) during reperfusion after ischemia preserved contractile function, possibly by inhibiting the JNK signaling pathway (35). Surprisingly, rMIF treatment of the perfused wild-type heart showed significant contractile depression similar to that reported previously by Garner *et al.* (15). Thus, it remains unclear whether exogenous rMIF delivered to the heart would serve a protective role during an ischemic event *in vivo*.

It is well recognized that ischemic myocardial injury triggers a local inflammatory response that results in the recruitment of leukocytes to the infarcted area (14). The potential role of MIF pro-inflammatory activity in leukocyte trafficking in this setting is not known, although neutralization of MIF in other disease models has been associated with reduced inflammation and monocyte recruitment (48). The present study focused on effects of MIF on tissue oxidative stress within a time frame that precludes effects on leukocyte recruitment. However, studies to examine the effect of MIF on postischemic cardiac remodeling may be warranted.

Development of drugs targeting the redox activity of MIF may provide benefit during oxidative stress without activating MIF pro-inflammatory activity. Similarly, small-molecule inhibitors of the pro-inflammatory or immune activities of MIF may provide therapeutic benefit without undesirable side effects on cardiac function. Because the effectiveness of MIF redox activity resides within the cell, one strategy may be to increase intracellular MIF by preventing its release during oxidative stress, or alternatively, to increase MIF uptake or expression (29, 45). MIF uptake into the cell can occur by endocytosis, which was recently reported to be facilitated by its association with cell-surface thioredoxin (41). Exploitation of this association may provide a mechanism to enhance intracellular availability of MIF.

In conclusion, our studies provide the first *in vivo* evidence supporting a role for the oxidoreductase function of MIF in mediating cardioprotection during ischemia and reperfusion by reducing the oxidative environment of the myocardium. Thus, therapeutic targeting of the redox activity of MIF has the potential to preserve cardiac function after ischemic injury.

Acknowledgments

We thank Drs. Koichiro Takahashi, Helena M. Linge, and YinZhong Zhang for their generosity in sharing ideas and expertise in developing experimental procedures. We are particularly indebted to Drs. Christine N. Metz and Yousef Al-Abed for their insightful discussion of this work.

This study was supported in part by a grant-in-aid from the American Heart Association Founders Affiliate (to K.O.).

Author Disclosure Statement

All authors state that no competing financial interests exist.

References

1. Ahsan MK, Lekli I, Ray D, Yodoi J, and Das DK. Redox regulation of cell survival by the thioredoxin superfamily: an implication of redox gene therapy in the heart. *Antioxid Redox Signal* 11: 2741–2758, 2009.
2. Al-Abed Y, Dabideen D, Aljabari B, Valster A, Messmer D, Ochani M, Tanovic M, Ochani K, Bacher M, Nicoletti F, Metz C, Pavlov VA, Miller EJ, and Tracey KJ. ISO-1 binding to the tautomerase active site of MIF inhibits its pro-inflammatory activity and increases survival in severe sepsis. *J Biol Chem* 280: 36541–36544, 2005.
3. Baugh JA and Bucala R. Macrophage migration inhibitory factor. *Crit Care Med* 30: S27–S35, 2002.
4. Bendrat K, Al-Abed Y, Callaway DJ, Peng T, Calandra T, Metz CN, and Bucala R. Biochemical and mutational investigations of the enzymatic activity of macrophage migration inhibitory factor. *Biochemistry* 36: 15356–15362, 1997.
5. Bolli R. Causative role of oxyradicals in myocardial stunning: a proven hypothesis: a brief review of the evidence demonstrating a major role of reactive oxygen species in several forms of postischemic dysfunction. *Basic Res Cardiol* 93: 156–162, 1998.
6. Bozza M, Satoskar AR, Lin G, Lu B, Humbles AA, Gerard C, and David JR. Targeted disruption of migration inhibitory factor gene reveals its critical role in sepsis. *J Exp Med* 189: 341–346, 1999.
7. Bulteau AL, Lundberg KC, Ikeda-Saito M, Isaya G, and Szweda LI. Reversible redox-dependent modulation of mitochondrial aconitase and proteolytic activity during in vivo cardiac ischemia/reperfusion. *Proc Natl Acad Sci U S A* 102: 5987–5991, 2005.
8. Buttke TM and Sandstrom PA. Oxidative stress as a mediator of apoptosis. *Immunol Today* 15: 7–10, 1994.
9. Calandra T, Echtenacher B, Roy DL, Pugin J, Metz CN, Hultner L, Heumann D, Mannel D, Bucala R, and Glauser MP. Protection from septic shock by neutralization of macrophage migration inhibitory factor. *Nat Med* 6: 164–170, 2000.

10. Calandra T and Roger T. Macrophage migration inhibitory factor: a regulator of innate immunity. *Nat Rev Immunol* 3: 791–800, 2003.
11. Chagnon F, Metz CN, Bucala R, and Lesur O. Endotoxin-induced myocardial dysfunction: effects of macrophage migration inhibitory factor neutralization. *Circ Res* 96: 1095–1102, 2005.
12. Dhanantwari P, Nadaraj S, Kenessey A, Chowdhury D, Al-Abed Y, Miller EJ, and Ojamaa K. Macrophage migration inhibitory factor induces cardiomyocyte apoptosis. *Biochem Biophys Res Commun* 371: 298–303, 2008.
13. Fingerle-Rowson G, Kaleswarapu DR, Schlander C, Kabgani N, Brocks T, Reinart N, Busch R, Schutz A, Lue H, Du X, Liu A, Xiong H, Chen Y, Nemajerova A, Hallek M, Bernhagen J, Leng L, and Bucala R. A tautomerase-null macrophage migration-inhibitory factor (MIF) gene knock-in mouse model reveals that protein interactions and not enzymatic activity mediate MIF-dependent growth regulation. *Mol Cell Biol* 29: 1922–1932, 2009.
14. Frangogiannis NG. Targeting the inflammatory response in healing myocardial infarcts. *Curr Med Chem* 13: 1877–1893, 2006.
15. Garner LB, Willis MS, Carlson DL, DiMaio JM, White MD, White DJ, Adams GAt, Horton JW, and Giroir BP. Macrophage migration inhibitory factor is a cardiac-derived myocardial depressant factor. *Am J Physiol Heart Circ Physiol* 285: H2500–H2509, 2003.
16. Halestrap AP, Clarke SJ, and Javadov SA. Mitochondrial permeability transition pore opening during myocardial reperfusion: a target for cardioprotection. *Cardiovasc Res* 61: 372–385, 2004.
17. Jones SP, Girod WG, Palazzo AJ, Granger DN, Grisham MB, Jourd'Heuil D, Huang PL, and Lefer DJ. Myocardial ischemia-reperfusion injury is exacerbated in absence of endothelial cell nitric oxide synthase. *Am J Physiol* 276: H1567–H1573, 1999.
18. Jones SP, Hoffmeyer MR, Sharp BR, Ho YS, and Lefer DJ. Role of intracellular antioxidant enzymes after in vivo myocardial ischemia and reperfusion. *Am J Physiol Heart Circ Physiol* 284: H277–H282, 2003.
19. Kenessey A, Sullivan EA, and Ojamaa K. Nuclear localization of protein kinase C-alpha induces thyroid hormone receptor-alpha1 expression in the cardiomyocyte. *Am J Physiol Heart Circ Physiol* 290: H381–H389, 2006.
20. Kim SH, Kang KA, Zhang R, Piao MJ, Ko DO, Wang ZH, Chae SW, Kang SS, Lee KH, Kang HK, Kang HW, and Hyun JW. Protective effect of esculetin against oxidative stress-induced cell damage via scavenging reactive oxygen species. *Acta Pharmacol Sin* 29: 1319–1326, 2008.
21. Kleemann R, Kapurniotu A, Frank RW, Gessner A, Mischke R, Flieger O, Juttner S, Brunner H, and Bernhagen J. Disulfide analysis reveals a role for macrophage migration inhibitory factor (MIF) as thiol-protein oxidoreductase. *J Mol Biol* 280: 85–102, 1998.
22. Kleemann R, Mischke R, Kapurniotu A, Brunner H, and Bernhagen J. Specific reduction of insulin disulfides by macrophage migration inhibitory factor (MIF) with glutathione and dihydrolipoamide: potential role in cellular redox processes. *FEBS Lett* 430: 191–196, 1998.
23. Kleemann R, Rorsman H, Rosengren E, Mischke R, Mai NT, and Bernhagen J. Dissection of the enzymatic and immunologic functions of macrophage migration inhibitory factor: full immunologic activity of N-terminally truncated mutants. *Eur J Biochem* 267: 7183–7193, 2000.
24. Kondo N, Ishii Y, Son A, Sakakura-Nishiyama J, Kwon YW, Tanito M, Nishinaka Y, Matsuo Y, Nakayama T, Taniguchi M, and Yodoi J. Cysteine-dependent immune regulation by TRX and MIF/GIF family proteins. *Immunol Lett* 92: 143–147, 2004.
25. Krause G, Lundstrom J, Barea JL, Pueyo de la Cuesta C, and Holmgren A. Mimicking the active site of protein disulfide-isomerase by substitution of proline 34 in *Escherichia coli* thioredoxin. *J Biol Chem* 266: 9494–9500, 1991.
26. Kumar D and Jugdutt BI. Apoptosis and oxidants in the heart. *J Lab Clin Med* 142: 288–297, 2003.
27. Lillig CH and Holmgren A. Thioredoxin and related molecules: from biology to health and disease. *Antioxid Redox Signal* 9: 25–47, 2007.
28. Lin X, Sakuragi T, Metz CN, Ojamaa K, Skopicki HA, Wang P, Al-Abed Y, and Miller EJ. Macrophage migration inhibitory factor within the alveolar spaces induces changes in the heart during late experimental sepsis. *Shock* 24: 556–563, 2005.
29. Miller EJ, Li J, Leng L, McDonald C, Atsumi T, Bucala R, and Young LH. Macrophage migration inhibitory factor stimulates AMP-activated protein kinase in the ischaemic heart. *Nature* 451: 578–582, 2008.
30. Murphy E and Steenbergen C. Mechanisms underlying acute protection from cardiac ischemia-reperfusion injury. *Physiol Rev* 88: 581-609, 2008.
31. Nagy N, Malik G, Tosaki A, Ho YS, Maulik N, and Das DK. Overexpression of glutaredoxin-2 reduces myocardial cell death by preventing both apoptosis and necrosis. *J Mol Cell Cardiol* 44: 252–260, 2008.
32. Nguyen MT, Beck J, Lue H, Funfzig H, Kleemann R, Koolwijk P, Kapurniotu A, and Bernhagen J. A 16-residue peptide fragment of macrophage migration inhibitory factor, MIF-(50-65), exhibits redox activity and has MIF-like biological functions. *J Biol Chem* 278: 33654–33671, 2003.
33. Nguyen MT, Lue H, Kleemann R, Thiele M, Tolle G, Finkelmeier D, Wagner E, Braun A, and Bernhagen J. The cytokine macrophage migration inhibitory factor reduces pro-oxidative stress-induced apoptosis. *J Immunol* 170: 3337–3347, 2003.
34. Noels H, Bernhagen J, and Weber C. Macrophage migration inhibitory factor: a noncanonical chemokine important in atherosclerosis. *Trends Cardiovasc Med* 19: 76–86, 2009.
35. Qi D, Hu X, Wu X, Merk M, Leng L, Bucala R, and Young LH. Cardiac macrophage migration inhibitory factor inhibits JNK pathway activation and injury during ischemia/reperfusion. *J Clin Invest* 119: 3807–3816, 2009.
36. Robin E, Guzy RD, Loor G, Iwase H, Waypa GB, Marks JD, Hoek TL, and Schumacker PT. Oxidant stress during simulated ischemia primes cardiomyocytes for cell death during reperfusion. *J Biol Chem* 282: 19133–19143, 2007.
37. Rosenkranz AR, Schmaldienst S, Stuhlmeier KM, Chen W, Knapp W, and Zlabinger GJ. A microplate assay for the detection of oxidative products using 2′,7′-dichlorofluorescein-diacetate. *J Immunol Methods* 156: 39–45, 1992.
38. Sakuragi T, Lin X, Metz CN, Ojamaa K, Kohn N, Al-Abed Y, and Miller EJ. Lung-derived macrophage migration inhibitory factor in sepsis induces cardio-circulatory depression. *Surg Infect (Larchmt)* 8: 29–40, 2007.
39. Schwalb H, Olivson A, Li J, Houminer E, Wahezi SE, Opie LH, Maulik D, Borman JB, and Powell SR. Nicorandil decreases postischemic actin oxidation. *Free Radic Biol Med* 31: 607–614, 2001.
40. Sherry B, Yarlett N, Strupp A, and Cerami A. Identification of cyclophilin as a proinflammatory secretory product of

lipopolysaccharide-activated macrophages. *Proc Natl Acad Sci U S A* 89: 3511–3515, 1992.
41. Son A, Kato N, Horibe T, Matsuo Y, Mochizuki M, Mitsui A, Kawakami K, Nakamura H, and Yodoi J. Direct association of thioredoxin-1 (TRX) with macrophage migration inhibitory factor (MIF): regulatory role of TRX on MIF internalization and signaling. *Antioxid Redox Signal* 11: 2595–2605, 2009.
42. Sun C, Li H, Leng L, Raizada MK, Bucala R, and Sumners C. Macrophage migration inhibitory factor: an intracellular inhibitor of angiotensin II-induced increases in neuronal activity. *J Neurosci* 24: 9944–9952, 2004.
43. Swope MD, Sun HW, Klockow B, Blake P, and Lolis E. Macrophage migration inhibitory factor interactions with glutathione and S-hexylglutathione. *J Biol Chem* 273: 14877–14884, 1998.
44. Tagaya Y, Maeda Y, Mitsui A, Kondo N, Matsui H, Hamuro J, Brown N, Arai K, Yokota T, Wakasugi H, *et al.* ATL-derived factor (ADF), an IL-2 receptor/Tac inducer homologous to thioredoxin; possible involvement of dithiol-reduction in the IL-2 receptor induction. *EMBO J* 8: 757–764, 1989.
45. Takahashi M, Nishihira J, Shimpo M, Mizue Y, Ueno S, Mano H, Kobayashi E, Ikeda U, and Shimada K. Macrophage migration inhibitory factor as a redox-sensitive cytokine in cardiac myocytes. *Cardiovasc Res* 52: 438–445, 2001.
46. Thum T, Gross C, Fiedler J, Fischer T, Kissler S, Bussen M, Galuppo P, Just S, Rottbauer W, Frantz S, Castoldi M, Soutschek J, Koteliansky V, Rosenwald A, Basson MA, Licht JD, Pena JT, Rouhanifard SH, Muckenthaler MU, Tuschl T, Martin GR, Bauersachs J, and Engelhardt S. MicroRNA-21 contributes to myocardial disease by stimulating MAP kinase signalling in fibroblasts. *Nature* 456: 980–984, 2008.
47. von Harsdorf R, Li PF, and Dietz R. Signaling pathways in reactive oxygen species-induced cardiomyocyte apoptosis. *Circulation* 99: 2934–2941, 1999.
48. Zernecke A, Bernhagen J, and Weber C. Macrophage migration inhibitory factor in cardiovascular disease. *Circulation* 117: 1594–1602, 2008.
49. Zhu X, Zuo L, Cardounel AJ, Zweier JL, and He G. Characterization of in vivo tissue redox status, oxygenation, and formation of reactive oxygen species in postischemic myocardium. *Antioxid Redox Signal* 9: 447–455, 2007.

Address correspondence to:
Kaie Ojamaa, Ph.D.
The Feinstein Institute for Medical Research
350 Community Drive
Manhasset, NY 11030

E-mail: kojamaa@nshs.edu

Date of first submission to ARS Central, February 19, 2010; date of final revised submission, August 26, 2010; date of acceptance, September 11, 2010.

Abbreviations Used

AAR = area at risk
AMPK = AMP-activated protein kinase
BCA = bicinchoninic acid
DCF-DA = 2′,7′-dichlorodihydrofluorescein diacetate
DNPH = 2,4-dinitrophenylhydrazone
DTNB = 5,5′-dithiobis-(2-nitrobenzoic acid)
DTT = dithiothreitol
GLUT = glucose transporter
Grx = glutaredoxin
GSH = glutathione
GSSG = glutathione disulfide
INF = infarct area
I/R = ischemia and reperfusion
JNK = c-Jun N-terminal kinase
KO = knockout
LCA = left coronary artery
LV = left ventricle
MIF = macrophage migration-inhibitory factor
Prx = peroxiredoxin
rMIF = recombinant MIF
RNS = reactive nitrogen species
ROS = reactive oxygen species
TPOR = thiol-protein oxidoreductase
Trx = thioredoxin
TTC = 2,3,5-triphenyl-tetrazolium chloride
WT = wild type

This article has been cited by:

1. Yan-Mei Zhang, Chun-Yan Wang, Fu-Chun Zheng, Fen-Fei Gao, Yi-Cun Chen, Zhan-Qin Huang, Zheng-Yuan Xia, Michael G. Irwin, Wei-Qiu Li, Xing-Ping Liu, Yan-Shan Zheng, Han Xu, Gang-Gang Shi. 2012. Effects of N-n-butyl haloperidol iodide on the rat myocardial sarcoplasmic reticulum Ca2+–ATPase during ischemia/reperfusion. *Biochemical and Biophysical Research Communications* **425**:2, 426-430. [CrossRef]
2. Claudia V Pereira, Sashi Nadanaciva, Paulo J Oliveira, Yvonne Will. 2012. The contribution of oxidative stress to drug-induced organ toxicity and its detection in vitro and in vivo. *Expert Opinion on Drug Metabolism & Toxicology* 1-19. [CrossRef]
3. C Stoppe, G Grieb, D Simons, R Rossaint, J Bernhagen, S Rex. 2012. High postoperative blood levels of macrophage migration inhibitory factor are associated with less organ dysfunction in patients after cardiac surgery. *Critical Care* **16**:Suppl 1, P471. [CrossRef]
4. Nic E. Savaskan, Günter Fingerle-Rowson, Michael Buchfelder, Ilker Y. Eyüpoglu. 2012. Brain Miffed by Macrophage Migration Inhibitory Factor. *International Journal of Cell Biology* **2012**, 1-11. [CrossRef]
5. Jingjun Lu , Sona Mitra , Xianwei Wang , Magomed Khaidakov , Jawahar L. Mehta . 2011. Oxidative Stress and Lectin-Like Ox-LDL-Receptor LOX-1 in Atherogenesis and Tumorigenesis. *Antioxidants & Redox Signaling* **15**:8, 2301-2333. [Abstract] [Full Text HTML] [Full Text PDF] [Full Text PDF with Links]
6. Jingjun Lü, Jawahar L. Mehta. 2011. LOX-1: A Critical Player in the Genesis and Progression of Myocardial Ischemia. *Cardiovascular Drugs and Therapy* . [CrossRef]
7. Xiaojie Xie, Yifan Wang, Songzhao Zhang, Guidi Zhang, Yinchuan Xu, Honghao Bi, Alan Daugherty, Jian-an Wang. 2011. Chinese red yeast rice attenuates the development of angiotensin II-induced abdominal aortic aneurysm and atherosclerosis. *The Journal of Nutritional Biochemistry* . [CrossRef]